PHYSICAL REVIEW C **83**, 041601(R) (2011)

Discrete deexcitations in ^{235}U below 3 MeV from nuclear resonance fluorescence

E. Kwan,[1,2,*] G. Rusev,[1,2] A. S. Adekola,[2,3,†] F. Dönau,[4] S. L. Hammond,[2,3] C. R. Howell,[1,2] H. J. Karwowski,[2,3] J. H. Kelley,[2,5] R. S. Pedroni,[2,6] R. Raut,[1,2] A. P. Tonchev,[1,2] and W. Tornow[1,2]

[1]*Department of Physics, Duke University, Durham, North Carolina 27708, USA*
[2]*Triangle Universities Nuclear Laboratory, Durham, North Carolina 27708, USA*
[3]*Department of Physics and Astronomy, University of North Carolina at Chapel Hill, Chapel Hill, North Carolina 27599, USA*
[4]*Institut für Strahlenphysik, Forschungszentrum Dresden Rossendorf, D-01314 Dresden, Germany*
[5]*Department of Physics, North Carolina State University, Raleigh, North Carolina 27695, USA*
[6]*Department of Physics, North Carolina A&T State University, Greensboro, North Carolina 27411, USA*

(Received 5 May 2010; revised manuscript received 11 January 2011; published 21 April 2011)

Gamma-ray transitions in ^{235}U were measured using the (γ, γ') reaction below 3 MeV. The nuclear-resonance-fluorescence experiment was carried out at the High-Intensity γ-ray Source facility using nearly monoenergetic and circularly polarized photon beams. More than 20 transitions corresponding to deexcitations to the ground state and low-lying levels in ^{235}U were observed. The integrated cross sections to the excited levels and intensities of branching transitions were deduced. The experimental results are compared with predictions from a quasiparticle random-phase approximation in a deformed basis.

DOI: 10.1103/PhysRevC.83.041601 PACS number(s): 23.20.Lv, 25.20.Dc, 27.90.+b

Low-lying collective $M1$ excitations known as the "scissors mode" have been observed in electron- and photon-scattering experiments on deformed nuclei [1,2]. The scissors mode exhibits strength proportional to the square of the ground-state deformation [3]. The systematics of the summed $M1$ reduced-transition probability, $\Sigma B(M1)$, in even-even mass, rare-earth isotopes at excitation energies of 2.5 to 4.0 MeV, indicates increasing strength for midshell nuclei and decreasing strengths for nuclei near shell closure and in the region of γ softness [3–5]. Theoretical calculations using the interacting boson-fermion [6,7] and quasiparticle-phonon nuclear models [8] predict sizable $M1$ strength in both odd-mass and even-even rare-earth nuclei. The actinide region is interesting for investigation of the scissors mode because it includes neutron-rich nuclei with large deformations. Calculations using quasiparticle random-phase approximation (QRPA) are able to predict the energy centroid and summed $B(M1)$ and $B(E1)$ strengths in ^{232}Th, ^{236}U, and ^{238}U [9,10], but more experimental information on the $\Sigma B(M1)$ strengths is needed in other actinide nuclei to determine the properties of the scissors mode.

The potential existence of strong nuclear dipole excitations in the actinides at γ-ray energies above 2 MeV is important for cargo interrogation, which requires a probe capable of penetrating shielding material of substantial thickness. The identification of γ-ray transitions from excited levels between about 2 MeV and the neutron-separation energy in special nuclear materials such as ^{235}U and ^{238}U will provide unique signatures useful for isotopic identification, which is necessary for developing nonintrusive interrogation technologies [11,12].

The low-momentum transfer in (γ,γ') reaction emphasizes dipole excitations and therefore is an excellent tool for investigating and characterizing low-spin electromagnetic transitions. Previous nuclear-resonance-fluorescence (NRF) measurements on the actinide isotopes ^{232}Th, ^{238}U [13,14], and ^{236}U [15] revealed $M1$ excitations concentrated around 2.0 to 2.5 MeV, whose $\Sigma B(M1)$ are comparable to the midshell, rare-earth nuclei [13]. Dipole deexcitations from states up to 2.1 MeV were observed in the ^{235}U nucleus in a (γ,γ') measurement using bremsstrahlung beams [16,17].

The detection of weak nuclear transitions is challenging in experiments using bremsstrahlung owing to the high background. The background radiation, which is mostly attributable to atomic scattering of the photon beam from the target, increases with the square of the atomic number. This does not favor NRF measurements on the actinides. In these nuclides, the transition strength becomes highly fragmented owing to the high level densities, and the large background from atomic scattering masks weak transitions. A significant reduction of the atomic background and a higher detection sensitivity can be achieved using monoenergetic photon beams such as those delivered by the High-Intensity γ-ray Source (HIγS) facility operated by the Triangle Universities Nuclear Laboratory. Energetic photon beams from HIγS are created by inverse Compton scattering of a high-intensity free-electron laser (FEL) light from an intense electron beam in a storage ring. Presently, the HIγS facility is capable of producing 100% linear or circular polarized photon beams in the energy range from 1 to 100 MeV with an energy spread from 0.5% to 5.0% [18].

In this Rapid Communication, results from a NRF experiment on ^{235}U are presented. The current measurements were carried out at the HIγS facility using nearly monoenergetic and circularly polarized beams with energies from 1.6 to 3.0 MeV. A 30.5-cm-long lead collimator with a cylindrical

*Present address: Lawrence Livermore National Laboratory, P.O. Box 808, Livermore, California 94551, USA.
†Present address: Department of Physics and Astronomy, Rutgers University, Piscataway, New Jersey 08854 USA.

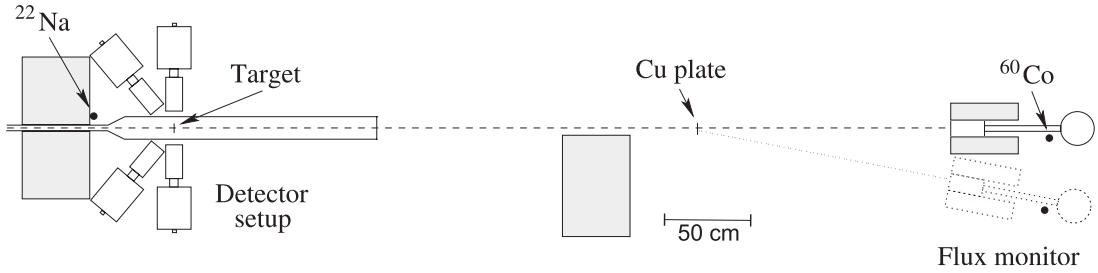

FIG. 1. The experimental-setup scheme showing the detectors in the horizontal plane and the large-volume HPGe detector used for monitoring the flux. The photon beam, whose central axis is represented by the dashed line, impinged the target placed in an evacuated pipe from the left. Lead shieldings are depicted by the shaded blocks and radioactive sources used to correct for the data acquisition's dead time and signal pileup effects are labeled. The position of the flux monitor at 11.3° is indicated by dotted lines.

hole of 1.905 cm in diameter, was positioned 60 m downstream from the collision point of the electrons with the FEL photons and upstream from the detector array. Owing to the inverse Compton-scattering mechanism, the energy spread of the photon beam depends on the collimator size. The diameter of the lead aperture was selected to provide photon beams with an energy spread of about 3% and ensured that the beam spot illuminating the ^{235}U foils was smaller than the surface area of the target. The ^{235}U targets consisted of two or three 0.03-cm-thick square foils, each with a surface area of 2.54×2.54 cm^2 and sealed with 0.01-cm-thick plastic laminates. The targets were enriched to 93.7% in ^{235}U with a total mass of 3.08 or 4.62 g. The targets were placed perpendicular to the incident photon beams inside an evacuated plastic pipe.

The scattered γ rays from the target were measured with a high-purity germanium (HPGe) detector array positioned 10 m downstream from the collimator. Shown in Fig. 1 is a schematic drawing of the experimental setup. Four HPGe detectors with 60% relative efficiency were placed 10 cm away from the center of the target at an angle of 90° relative to the beam. Two of these detectors were located in the horizontal plane and the other two in the vertical plane. Lead and copper absorbers with thicknesses of 3.2 and 4.0 mm, respectively, were mounted on the front face of these detectors to attenuate the intensity of the low-energy, atomic-scattering background. The array included two additional HPGe detectors with 25% relative efficiency. These detectors equipped with 1.8-mm-thick lead absorbers were positioned symmetrically about the incident photon beam axis in the horizontal plane at backward angles of 140° and at a distance of 13.2 cm from the center of the target. The detector array was shielded from small-angle-scattered photons originating from the collimator by 60 cm of concrete and three lead walls with a total thickness of 85 cm (the first two walls are not shown in Fig. 1). Multichannel analyzers providing spectra with resolution of 0.2 keV/channel processed the energy signals. A typical acquisition dead time of 15% at 5 kcps was estimated using a ^{22}Na source positioned in the vicinity of the detector array (cf. Fig. 2).

The energy distributions of the incident photons were measured using a large-volume HPGe detector with a relative efficiency of 123% positioned in the beam. To not overload this detector, copper absorbers located at the exit of the FEL were used to attenuate the beam and were positioned about 40 m upstream of the detector array to minimize the distortion from small-angle scattered photons. Shown in Fig. 2(a) is the measured beam profile with a centroid energy of $E_\gamma \sim 2.1$ MeV and energy spread of about 3%. Simulations with GEANT3 [19] were used to correct the measured beam energy spectra for the detector response. The efficiency of the detector for a photon beam collimated by a lead block with a 1.905-cm hole was also simulated. The kinematics of inverse Compton scattering, that is, the angle-energy correlation of the photon beam [20], was explicitly taken into account in the simulations.

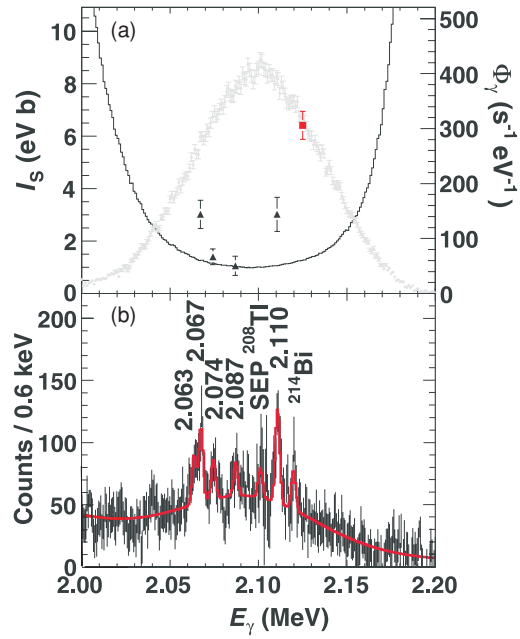

FIG. 2. (Color online) (a) Spectrum of the incident flux $\Phi_\gamma(E_\gamma)$ of the photon beam compared with the value deduced from a measurement with a ^{11}B target (the red square). The integrated cross sections deduced from the ^{235}U target at the same beam energy, represented by the filled triangles vs the detection sensitivity (histogram) is also shown. (b) The measured spectrum from a ^{235}U target at a photon energy of 2.1 MeV after subtraction of the natural background from the target. The vertical lines depict the statistical uncertainties. The red curve is a fit to the spectrum, and the energies of the transitions from ^{235}U are labeled.

The unattenuated photon flux was monitored during the actual NRF measurements on ^{235}U by the same large-volume HPGe detector, but now placed at an angle of 11.3° relative to the beam axis. Photons scattered into this detector by a 1-mm-thick copper plate positioned perpendicular to the beam axis and at a distance of 147 cm (cf. Fig. 1) from the HPGe detector were detected at a rate suitable for this detector. The measured spectrum of the Compton-scattered photons was also corrected for the detector response, as discussed above, to deduce the peak area. The absolute flux was determined using the measured yields and the Compton scattering cross sections calculated using the Klein-Nishina formula [21]. The absolute efficiency of the HPGe detector used to monitor the beam flux was measured using ^{56}Co, ^{88}Y, and ^{152}Eu γ-ray calibration sources, which were mounted on the downstream side of the copper plate. These extended sources had a diameter of 2 cm, similar to the incident photon beam. A ^{60}Co source was positioned behind the detector (cf. Fig. 1) to determine the dead time, typically 5% at a rate of 2 kcps, of the data acquisition and pile up losses, analogously to what was done for the HPGe detector array.

The method for determining the photon flux was cross-checked by a measurement on ^{11}B at a beam energy of 2.1 MeV. A 2.15-g ^{11}B cylinder enriched to 99.52% with diameter of 2.86 cm was used to determine the incident flux from exciting the 2.125-MeV state in ^{11}B. The photon flux, $\Phi_\gamma(E_\gamma)$, was determined from solving the integrated cross section I_S formula given by

$$I_S = \frac{A}{t W(\theta) n_t \Phi_\gamma(E_\gamma) \epsilon(E_\gamma) T(E_\gamma)}, \qquad (1)$$

where A is the full-energy peak area of the ground-state transition measured during the elapsed time t corrected for the data acquisition's dead time, n_t is the areal density of the target, $W(\theta)$ is the angular distribution at angle θ relative to the beam, and $T(E_\gamma)$ is the γ-ray transmission probability through the target. The full-energy peak efficiency of the detector array, $\epsilon(E_\gamma)$, was deduced by measurements using ^{54}Mn, ^{56}Co, ^{60}Co, ^{88}Y, ^{133}Ba, ^{152}Eu, and ^{226}Ra calibration sources up to $E_\gamma = 3.5$ MeV. In the case of the ground-state transition from the ^{11}B $E_x = 2.125$ MeV level, the angular distribution has previously been observed to be isotropic [22]. The photon flux deduced from the transition in ^{11}B is plotted in Fig. 2(a) as a red square and compared with the values determined from the measurement of Compton scattered photons from the copper plate referred to above.

In the present investigation, discrete deexcitations in ^{235}U below 3 MeV were determined from 14 measurements with beam energies centered between 1.6 and 3.0 MeV in steps of about 0.1 MeV. The ambient radiation from the room and the uranium targets were subtracted from the summed spectra of the HPGe detector array at each beam energy to describe the remaining background with known physical processes. Displayed in Fig. 2(b) is an example of such a spectrum from the (γ,γ') reaction on ^{235}U at a beam energy of 2.1 MeV. The remaining background in the corrected spectrum in the energy range of the photon beam is attributed to Rayleigh, Thomson, and Delbrück scattering of the incident photons from the target (see, e.g., Refs. [23,24]). Therefore, a decaying exponential function representing the atomic background at lower energies and the shape of the beam-energy distribution, which is proportional to the intensity owing to elastic scattering, were used as the fit to the remaining background. The peaks were then fitted using ROOT [25] at a binning of 0.6 keV/channel with Gaussians with widths fixed based on the full width at half maximum of the strong background transitions whose resolution was found to be 2.9 keV at 2100 keV.

In Fig. 2(b), transitions observed from ^{235}U at a beam energy of 2.1 MeV are labeled with their energies given in MeV. The background corrected in-beam spectra were compared to the spectrum resulting from the natural activity of the target to investigate whether there are residual counts from background peaks. Two such peaks corresponding to the single-escape peak from the transition at 2.615 MeV in ^{208}Tl and the 2.119-MeV transition in ^{214}Bi are labeled. The 6.3% ^{238}U contamination in the target may result in the presence of additional background peaks. These peaks can be identified from NRF measurements on a ^{238}U target [26].

The I_S for populating levels in ^{235}U were determined according to Eq. (1). GEANT3 simulations were performed for γ rays emitted isotropically in the volume of the target to estimate their attenuation in the target. From the simulations it was determined that for the 3.08-g target, the transmission varied slowly from 78.6% to 80.6% for 90° and 97.4% to 98.0% for 140°, at photon energies of 1.6 and 3.0 MeV, respectively.

Corrections to the measured intensities owing to the self-absorption were also taken into account. A non-negligible notch in the photon-flux distribution as a result of the nuclear absorption has been observed in heavy nuclei [12]. The correction for the nuclear self-absorption [27] assuming an effective temperature of 300 K was estimated to be 2.8% for a level with width $g\Gamma_0^2/\Gamma = 19.2$ meV at $E_\gamma = 1.73$ MeV. The results for the ground-state transitions from the present photon-scattering experiment are summarized in Table I. The level energies have been deduced from the weighted average of all transitions deexciting the level assuming the Ritz's combination principle.

The deexcitations in ^{235}U are typically weak and to distinguish them from the background fluctuations, the corresponding peak areas were compared with the detection limits. The detection limit represents the smallest peak area which can be considered as a real deexcitation. We used the expression given in Ref. [28] to deduce the detection limit, $A_{\rm DL}$, for a 2σ confidence level $A_{\rm DL} = 3.3\sqrt{2B}$, where B is the area of the background integrated over two times the typical dispersion of a peak in the same energy region. The detection limits were converted to I_S according to Eq. (1) and compared with the deduced values for the levels in ^{235}U [cf. Fig. 2(a)]. The values of I_S for ground-state transitions listed in Table I are larger than the detection limits.

In addition to the nine previously reported transitions from ^{235}U [16], 13 more transitions were observed for the first time. Two of transitions at 1974 and 2086 keV also coincide with known dipole states in ^{236}U. These transitions are unlikely to originate from ^{236}U, bec ause the Γ_0^2/Γ intensities do not agree

TABLE I. Transitions observed from ^{235}U in the present work. The integrated cross sections, widths, and intensity ratios relative to the intensity of the ground-state transition determined in this work are given.

E_x [a] (keV)	E_γ [b] (keV)	J_f^π [c]	I_S [d] (eVb)	$\frac{g\Gamma_0^2}{\Gamma}$ [e] (meV)	R [f]
1656.3(7)	1656.4(7)	$7/2^-$	3.0(11)	2.1(8)	1
1733.6(2)	1687.0(5)	$9/2^-$			0.6(2)
	1733.6(2)	$7/2^-$	22(4)	17(3)	1
1769.3(4)	1769.3(4)[g]	$7/2^-$	6.4(15)	5.2(12)	1
1815.2(2)	1769.3(4)[g]	$9/2^-$			0.62(4)
	1815.2(2)	$7/2^-$	8.9(11)	7.7(9)	1
1827.7(2)	1782.1(6)[h]	$9/2^-$			0.45(18)
	1827.6(2)	$7/2^-$	5.5(13)	4.8(12)	1
1862.4(1)	1862.4(1)	$7/2^-$	9.6(7)	8.7(7)	1
1973.8(3)	1973.8(3)	$7/2^-$	4.6(6)	4.7(6)	1
2003.3(2)	1957.4(2)	$9/2^-$			0.62(13)
	2003.0(3)	$7/2^-$	6.7(12)	7.0(13)	1
2005.9(4)	2005.9(4)	$7/2^-$	4.6(9)	4.8(9)	1
2010.6(3)	2010.6(3)	$7/2^-$	3.0(5)	3.2(6)	1
2067.1(4)	2067.1(4)	$7/2^-$	3.0(5)	3.4(6)	1
2074.2(3)	2074.2(3)	$7/2^-$	1.4(3)	1.5(4)	1
2086.7(6)	2086.7(6)	$7/2^-$	1.1(4)	1.2(4)	1
2110.2(3)	2063.3(6)	$9/2^-$			0.51(13)
	2110.4(3)	$7/2^-$	3.0(7)	3.5(8)	1
2216.1(3)	2216.1(3)	$7/2^-$	2.8(5)	3.6(6)	1
2416.1(3)	2416.1(3)	$7/2^-$	3.6(6)	5.4(9)	1
2555.6(6)	2555.6(6)	$7/2^-$	2.5(6)	4.3(10)	1
2754.7(4)	2754.7(4)	$7/2^-$	3.6(6)	7.2(11)	1

[a]Level energy determined from the weighted mean of all transitions deexciting this level assuming the Ritz's combination principle. The transition energies were corrected for recoil.
[b]Transition energy.
[c]Spin and parity of the final state.
[d]Integrated cross sections.
[e]Product of the statistical factor for the ground-state transition, $g = (2J_x + 1)/8$, and Γ_0^2/Γ, where Γ and Γ_0 are the total and ground-state widths, respectively.
[f]Transition intensity relative to the intensity of the ground-state transition.
[g]Possible ground-state or branching transition.
[h]Unresolved with a 1782-keV transition in ^{238}U.

with those reported in Ref. [15] and we do not expect any ^{236}U contamination in our targets.

Branching transitions from a particular level to low-lying states in ^{235}U were identified from the energy differences of the observed peaks and requiring that the branching transition has to be outside of the beam-energy distribution. Six transitions were observed from 1687 to 1827 keV at the photon energy of 1.8 MeV. Bertozzi *et al.* suggested that the two resonance peaks observed at 1687 and 1769 keV could be transitions to the 46-keV state and the 1734-keV line may be a ground-state transition. Their assignments were based on the assumption that both populated levels also have transitions to the 46-keV-state partner, but the continuous energy distribution of the bremsstrahlung beam used by Bertozzi *et al.* does not allow for a clear distinction between ground-state and branching transitions.

In the current work, we populated the level at 1734 keV using quasimonoenergic beams with energies of 1.7 and 1.8 MeV. We deduced integrated cross sections of 20(4) and 25(5) eV b, respectively, verifying that the 1734-keV peak is only a transition to the ground state. The weighted average of I_s for this state is listed in Table I. In addition, we observed a peak populated below the 1.8-MeV beam distribution at 1687 keV, suggesting that this transition is a branch to the 46-keV state from the 1734-keV level. A peak at 1769 keV, observed in the spectrum measured at beam energy of 1.8 MeV, can be considered as a ground-state transition from a level at 1769 keV because it is within the beam distribution. However, this peak is a candidate for a branching transition from the level at 1815 keV to the third excited state in ^{235}U at 46 keV. We cannot clearly assign the origin of the peak at 1769 keV from our experiment; therefore, we give the two options in Table I.

Calculations based on the QRPA are commonly used for interpretation of low-lying strength observed in NRF experiments. Although QRPA cannot predict the exact location and strength in deformed nuclei, it is an appropriate model to study the gross features of dipole-strength distributions. We applied a QRPA model based on an empirical mean field with a deformed Woods-Saxon potential. The RPA part consists of a residual interaction of the spin-spin type for calculating the $M1$ properties and a dipole-dipole interaction for the $E1$ properties. The deformation parameter for ^{235}U were taken from Ref. [29]. The spurious modes were eliminated by applying the method of mode suppression [30]. The same strength parameters as in Ref. [31] were taken for the spin-spin interaction. The strength parameters for the dipole-dipole interaction were derived analogously as in the QRPA calculations of the $E1$ strengths [32,33] in the deformed Mo isotopes and in the spherical $N = 50, 82$ isotones [34,35]. Results from the QRPA calculations for $M1$ and $E1$ strength in ^{235}U are compared with the experimental results in Fig. 3. For convenience, the theoretical results were converted to I_S in

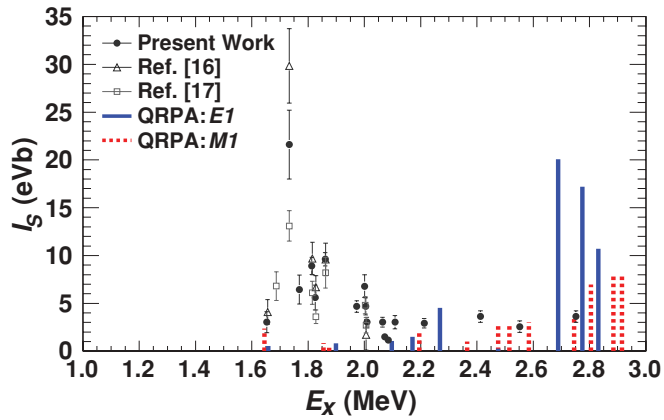

FIG. 3. (Color online) Predictions from QRPA model in deformed basis for the $M1$ (solid blue bars) and $E1$ (dashed red bars) strength in ^{235}U compared with the results from the present work (black data points) and Refs. [16,17] (open symbols).

Fig. 3 because the spin and parity could not be determined in the present experiment. The summed strength from the QRPA calculations $\Sigma I_S = 98$ eV b below 3 MeV agrees with the strength of $\Sigma I_S = 95(5)$ eV b determined from the discrete transitions observed in the present experiment. In addition, the strengths from our measurement are in agreement with those deduced in Ref. [16] to within statistical uncertainties and are systematically higher than the ones listed in Ref. [17] by about 30%, as can be seen in Fig. 3. The QRPA calculations predict that a significant part (42%) of the dipole strength is attributable to $E1$ transitions. Using this result as a benchmark, we can estimate that the experimentally observed $M1$ strength from 1.6 to 3.0 MeV would result in a $\Sigma B(M1)\uparrow$ of $0.30\mu_N^2$. This is comparable to the values of the $\Sigma B(M1)$ from 2.5 to 4.0 MeV in the odd-mass heavy deformed rare-earth nuclei around $A = 160$ and much smaller than the $\Sigma B(M1)\uparrow \approx 3\mu_N^2$ determined for the even-even mass rare-earth nuclei (cf. Ref. [2]).

In summary, we have performed measurements on the ^{235}U(γ,γ') reaction at the HIγS facility using nearly monoenergetic beams with energies from 1.6 to 3.0 MeV in steps of around 0.1 MeV. The high sensitivity achieved in the present experiment owing to the low level of atomic background allowed us to identify 13 discrete deexcitations for the first time, including 10 to the ground state, 2 branching transitions to the third excited states at 46.2 keV, and 1 unresolved transition in ^{235}U. The integrated cross sections and the relative intensities were deduced. The QRPA calculations are unable to reproduce the locations the observed transitions especially below 2 MeV, where the strongest transitions were found, suggesting that more theoretical and experimental work is needed for heavy odd-mass nuclei to understand the dipole excitations.

The authors would like to thank LANL and in particular R. O. Nelson for loaning us the ^{235}U targets and J. R. Tompkins for his assistance during the measurements. This work was supported in part by the DHS and DOE under Grants No. 2008-DN-077-ARI010, No. 2008-DN-077-ARI014, No. DE-FG02-97ER41033, and No. DE-FG02-97ER41.

[1] D. Bohle *et al.*, Phys. Lett. B **137**, 27 (1984).
[2] U. Kneissl *et al.*, Prog. Part. Nucl. Phys. **37**, 349 (1996).
[3] W. Ziegler, C. Rangacharyulu, A. Richter, and C. Spieler, Phys. Rev. Lett. **65**, 2515 (1990).
[4] J. Enders, P. vonNeumann-Cosel, C. Rangacharyulu, and A. Richter, Phys. Rev. C **71**, 014306 (2005).
[5] P. von Brentano *et al.*, Nucl. Phys. A **577**, 191c (1994).
[6] P. V. Isacker and A. Frank, Phys. Lett. B **225**, 1 (1989).
[7] Y. D. Devi and V. K. B. Kota, Nucl. Phys. A **600**, 20 (1996).
[8] V. G. Soloviev, A. V. Sushkov, and N. Y. Shirikova, Phys. Rev. C **53**, 1022 (1996).
[9] R. Nojarov *et al.*, Nucl. Phys. A **563**, 349 (1993).
[10] A. A. Kuliev *et al.*, Eur. Phys. J. A **43**, 313 (2010).
[11] W. Bertozzi and R. J. Ledoux, Nucl. Instr. Methods Phys. Res. B **1241**, 820 (2005).
[12] C. A. Hagmann *et al.*, J. Appl. Phys. **106**, 084901 (2009).
[13] R. D. Heil *et al.*, Nucl. Phys. A **476**, 39 (1988).
[14] A. Zilges *et al.*, Phys. Rev. C **52**, R468 (1995).
[15] J. Margraf *et al.*, Phys. Rev. C **42**, 771 (1990).
[16] W. Bertozzi *et al.*, Phys. Rev. C **78**, 041601(R) (2008).
[17] O. Yevetska *et al.*, Phys. Rev. C **81**, 044309 (2010).
[18] H. R. Weller *et al.*, Prog. Part. Nucl. Phys. **62**, 257 (2009).
[19] CERN Program Library Long Writeup W5013, Geneva, 1993 (unpublished).
[20] C. Sun, J. Li, G. Rusev, A. P. Tonchev, and Y. K. Wu, Phys. Rev. Spec. Top.–Accel. Beams **12**, 062801 (2009).
[21] G. F. Knoll, *Radiation Detection and Measurement* (Wiley & Sons, New York, 2000).
[22] G. Rusev *et al.*, Phys. Rev. C **79**, 047601 (2009).
[23] W. Mückenheim and M. Schumacher, J. Phys. (London) G **6**, 1237 (1980).
[24] M. Schumacher *et al.*, Z. Phys. A **300**, 193 (1981).
[25] R. Brun and F. Rademakers, Nucl. Instrum. Methods Phys. Res., Sect. A **389**, 81 (1997).
[26] S. L. Hammond *et al.* (unpublished).
[27] W. D. Hamilton (editor), *The Electromagnetic Interaction in Nuclear Spectroscopy* (North-Holland, Amsterdam, 1975).
[28] R. Jenkins, R. W. Gould, and D. Gedke, *Quantitative X-Ray Spectroscopy* (Dekker, New York, 1995).
[29] P. Möller *et al.*, At. Data Nucl. Data Tables **59**, 185 (1995).
[30] F. Dönau, Phys. Rev. Lett. **94**, 092503 (2005).
[31] G. Rusev *et al.*, Phys. Rev. C **73**, 044308 (2006).
[32] G. Rusev *et al.*, Phys. Rev. C **79**, 061302(R) (2009).
[33] F. Dönau *et al.*, Phys. Rev. C **76**, 014317 (2007).
[34] N. Benouaret *et al.*, Phys. Rev. C **79**, 014303 (2009).
[35] A. Makinaga *et al.*, Phys. Rev. C **82**, 024314 (2010).